Numerical Simulation and Wall Shear Stress Analysis of Pulsed Flow in a Cylindrical Pipe for a Cleaning in Place Process

Pichitra Uangpairoj[1*] and Kontorn Chamniprasart[1]

[1] School of Mechanical Engineering, Institute of Engineering, Suranaree University of Technology, Nakhon Ratchasima, Thailand 30000

* Corresponding Author: E-mail: pichitrau@hotmail.com

Abstract

Pulsed flow has the effect of raising the maximum wall shear stress which is one parameter of cleaning enhancement in cleaning in place (CIP) system. Thus, types of pulsed flow are considered to improve the cleaning efficiency of CIP system. To indicate the cleaning efficiency of pulsed flows, wall shear stresses of various types of pulsed flow in cylindrical pipe were investigated by using finite volume method of the commercial computational fluid dynamics code (FLUENT®). As a result of the study, there are some differences of mean wall shear stresses between the numerical simulations and the experimental data. These wall shear stresses were generated by pulsed flows whose velocity varies with time as sine function. Additionally, the numerical simulations of various types of pulsed flow showed that wall shear stress corresponds to the velocity inlet function. Mean wall shear stress is proportional to mean velocity inlet, amplitude and frequency of pulsation. Maximum wall shear stress and frequency of wall shear stress are also proportional to amplitude and frequency, respectively. Therefore, only wall shear stress analysis is not enough to indicate the cleaning efficiency of different type of pulsed flow.

Keywords: Computational fluid dynamics (CFD), Pulsed flow, Wall shear stress

1. Introduction

During thermal treatment in dairy industry, there is an undesired build-up of deposits on the surfaces of pipes and equipments, especially heat exchangers. The undesired deposits, fouling, can be created when denatured protein in milk, especially β-lactoglobulin and some saturated mineral deposit on the heat transfer surface [3].

Build-up of fouling reduces heat transfer because an insulated property of the fouling increases the heat resistance at the heat transfer surface. This effect leads to energy losses in dairy thermal system. Fouling also increases the pressure drop due to the increase in surface roughness and the decrease in cross section area of the flow channels [11]. For safety impact, fouling is the

Nomenclature

$C_{1\varepsilon}, C_{2\varepsilon}$, ผิดพลาด! ไม่ได้กำหนดที่คั่นหน้า a, b constants	
f	frequency (Hz)
k	the turbulent kinetic energy (J)
r	the rate constant
t	time (s)
S	the deformation tensor
S_{ij}	the mean strain rate (s^{-1})
$u(t)$	instantaneous velocity (m/s)
$\bar{u}$	average velocity (m/s)
u_p	amplitude velocity (m/s)
u	velocity component (m/s)
u'	fluctuating components (m/s)
x	Cartesian coordinate

Greek symbols

$\alpha_k, \alpha_\varepsilon$	the inverse effective Prandtl numbers for k and ε, respectively
ε	turbulent dissipation rate (W.kg^{-1})
η_0, β	the coefficients
δ	the kronecker delta
ρ	density (kg/m^3)
μ	dynamic viscosity (kg.m^{-1}.s^{-1})
μ_t	turbulent viscosity (kg.m^{-1}.s^{-1})
τ_w	wall shear stress (Pa)

Subscripts

i, j, k	equal to 1, 2 and 3 which correspond to x, y, z in Cartesian coordinate

source of contamination in dairy product because of the accumulation of microorganisms. Fouling is used to protect microorganisms from cleaning, especially thermophile microorganisms [7]. These problems lead to an attempt of fouling reduction. The deposits can be reduced by modifying the geometry of heat exchangers (especially in plate heat exchangers) [10] and surface properties of heat exchanger [13].

Cleaning in place (CIP) is one part of cleaning systems which is used in large-scale production. In the CIP system, chemicals in the solution tanks are circulated through the equipments by a supply pump. The flow circuit is regulated by the pneumatic valves. At the same time, pressure and temperature are recorded in order to check the progress of cleaning. Typically, there are five basic steps in the cleaning procedure: 1. Prerinse – rising with water to remove loosely bound substances from the surface; 2. Cleaning – removal of the deposit from the surface by the chemicals. In this step, the deposit is swollen after react with the chemicals. Then, the swollen deposit is removed from the surface by shear forces and diffusion; 3. Interrinse – removal and rinsing away of the chemicals from the surface; 4. Sanitizing – rinsing with the sanitizer to inactivate microorganisms; 5. Postrinse – removal of sanitizer with water from the system.

The cleaning efficiency is affected by chemical concentration, temperature and fluid flow [4]. Therefore, one way to enhance the cleaning is fluid flow adjustment. Gillham et al. [5] studied the effect of pulsed flow on cleaning enhancement of whey protein soil in tube. The results of this study show that pulsing both increases the rate of cleaning and changes cleaning rate behavior. Because reverse flow, generated by pulsed flow, can increase wall

shear stress. There is another study that related to Gillham's study. Blel et al. [2] studied the effect of turbulent pulsating flow to the bacteria removal in straight pipe. Pulsed flow can reduce the number of bacteria more than steady flow. The bacteria removal is affected by the combination of amplitude and frequency of pulsating flow. Moreover, the recirculation of pulsating flow induces high fluctuating shear rate at the wall. This effect can enhance deposit removal as same as Gillham's study

Wall shear stress affects on the cleaning rate as show in Table. 1. Thus, wall shear stress could be considered as one parameter which is used to indicate the cleaning efficiency of flows.

Table 1 Models Expressing the effect of wall shear stress on cleaning rates.

Relation	Wall shear stress range (Pa)	
$r = a + b\tau_w$	1-14	[14]
$\ln r = a + b\tau_w$	0.19-7.5	[6]
$\ln r = a - b\ln\tau_w$	0.8-1.3	[9]
$\ln r = a - b\tau_w$	1-50	[8]

In this study, a commercial computational fluid dynamics (CFD) code (FLUENT®) was employed to predict the shear stresses, generated by pulsed flow at the wall of pipe, compare with the experimental data which was measured by Blel et al [1]. The effects of amplitude, frequency and type of pulsed flow on wall shear stress were investigated as well. The expected results might be useful for the cleaning in place enhancement in pipe and tubular heat exchanger which is normally used in dairy process.

2. Material and Method

2.1 Flow domain and computational mesh

To investigate wall shear stress of pulsed flow by using commercial CFD code, fluid was flowed in a cylindrical pipe (23 mm inner diameter and 1630 mm length) made of stainless steel (average absolute roughness $0.3\pm0.05\mu m$). The cylindrical pipe was separated into 3 zones (zone1 690 mm lengths, zone2 250 mm lengths and zone3 690 mm lengths) as in Fig.1. Wall shear stresses were investigated in zone2 in order to eliminate the entrance and exit effects as same as the experiment [1]. The entire flow domain was created from blocks of hexahedral and wedge mesh elements in GAMBIT^{TM}. The total number of mesh elements is 228,852 elements. Non-uniform mesh in the radial direction was performed to satisfy the y^+ value limits ($y^+<5$) valid for the enhance-wall treatment which was used for wall shear stress analysis as in Fig.2.
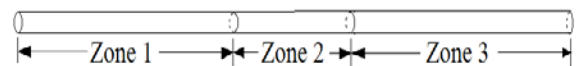

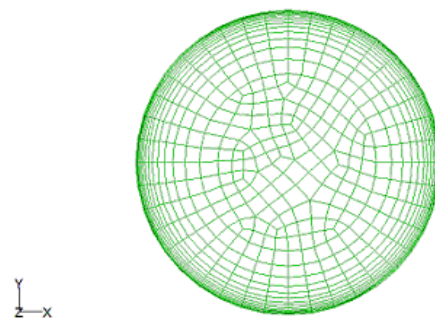Fig.1 Flow domain (the cylindrical pipe with 23 mm inner diameter and 1630 mm length).

Fig.2 Example of hexahedral and wedge mesh elements in the radial direction of flow domain.

At the inlet of cylindrical pipe, fluid flowed with velocity as show in Table. 2. The turbulence inlet conditions were set as

turbulence intensity and a hydraulic diameter. The turbulence intensity varied with the mean velocity of pulsed flow. The outlet was set as outflow boundary and no-slip conditions were applied to the wall. In the comparison between the numerical data and the experimental data, fluid material was assigned to be electrolytic solution. The density of the solution is 1028 kg/m^3 and its dynamics viscosity is 0.985 x 10^{-3} Pa.s. Meanwhile, water was adopted for the analysis of wall shear stresses that are generated by various type of pulsed flow.

Table 2 Hydrodynamic parameters for each pulsation condition

No.	Mean velocity (m/s)	Amplitude of the pulsations (m/s)	Frequency of the pulsations (Hz)
A	1.47	0.40	2.50
B	1.21	0.73	2.50
C	1.03	0.60	2.86
D	1.02	0.81	1.66
E	0.78	0.73	2.50
F	1.02	0.20	1.66
G	1.02	0.40	1.66
H	1.02	0.50	1.66
I	1.02	0.60	1.66
J	1.02	0.70	1.66
K	1.02	0.81	2.86
L	1.02	0.81	2.50
M	1.02	0.81	1.00
N	1.47	0.00	0.00
O	1.02	0.73	2.50
P	1.54	0.73	2.50

2.2 Computational Methods

The finite volume method of CFD code (FLUENT®) was employed to investigate wall shear stress of pulsating flow in cylindrical pipe. Steady and unsteady conditions were assumed for turbulent steady flow and turbulent pulsating flow, respectively. The velocity inlet could set as a constant and periodic function as in Eq. (1)-(4) for steady flow and pulsating flow, respectively.

Sine wave: $u(t) = \bar{u} + u_p \sin(2\pi f t)$ (1)

Square wave:

$$u(t) = \bar{u} + \frac{2u_p}{\pi}\sum_{n=1}^{\infty}\left(\frac{1-\cos n\pi}{n}\right)\sin e(2n\pi f) \quad (2)$$

Triangular wave:

$$u(t) = \bar{u} + \frac{8u_p}{\pi^2}\sum_{n=1}^{\infty}\left(\frac{1}{n^2}\sin\left(\frac{n\pi}{2}\right)\right)\sin e(2n\pi f) \quad (3)$$

Saw tooth wave:

$$u(t) = \bar{u} + \frac{2u_p}{\pi}\sum_{n=1}^{\infty}\left(\frac{\cos n\pi}{n}\right)\sin e(2n\pi f) \quad (4)$$

In this study, fluid was assumed to be constant object property and incompressible. Pipe was laid on horizon level; the effect of gravitation could be ignored. Flow was performed under isothermal condition.

The numerical model was based on solving the conservation of mass, momentum of turbulent flow which can be written in the Cartesian form of Reynolds-averaged Navier-Stokes equations as in Eq. (5)-(6).

ผิดพลาด! ไม่ได้กำหนดที่คั่น

$$\text{หน้า} \quad \frac{\partial \rho}{\partial t} + \frac{\partial}{\partial x_i}(\rho u_i) = 0 \quad (5)$$

$$\frac{\partial}{\partial t}(\rho u_i) + \frac{\partial}{\partial x_j}(\rho u_i u_j) =$$

$$-\frac{\partial p}{\partial x_i} + \frac{\partial}{\partial x_j}\left[\mu\left(\frac{\partial u_i}{\partial x_j} + \frac{\partial u_j}{\partial x_i} - \frac{2}{3}\delta_{ij}\frac{\partial u_l}{\partial x_l}\right)\right] \quad (6)$$

$$+ \frac{\partial}{\partial x_j}\left(-\rho\overline{u_i' u_j'}\right)$$

The Reynolds stress, $-\rho\overline{u_i' u_j'}$, can be related to the mean velocity gradients by using Boussinesq hypothesis as in Eq. (7).

$$-\rho\overline{u_i' u_j'} = \mu_t\left(\frac{\partial u_i}{\partial x_j} + \frac{\partial u_j}{\partial x_i}\right) \\ -\frac{2}{3}\left(\rho k + \mu_t\frac{\partial u_k}{\partial x_k}\right)\delta_{ij} \quad (7)$$

The turbulent viscosity, μ_t, in Eq. (7) can be determined from turbulent kinetic energy, k, and turbulent dissipation rate, ε. Both of k and ε are obtained from RNG k-ε model in Eq. (8)-(9) which was more accurate and reliable for a wider class of flows than the standard k-ε model, especially for prediction of the wall shear stress [7]. Due to the k-ε models are not valid in the near wall region. Thus, enhance wall treatment was added to captured flow behavior in viscous sub-layer.

$$\rho\frac{Dk}{Dt} = \frac{\partial}{\partial x_j}\left(\alpha_k\mu_{eff}\frac{\partial k}{\partial x_j}\right) + \mu_t S^2 - \rho\varepsilon_k \quad (8)$$

$$\rho\frac{D\varepsilon}{Dt} = \frac{\partial}{\partial x_j}\left(\alpha_\varepsilon\mu_{eff}\frac{\partial\varepsilon}{\partial x_j}\right) \\ + \frac{\varepsilon}{k}\left(C_{1\varepsilon}\mu_t S^2 - \rho C_{2\varepsilon}^*\varepsilon\right) \quad (9)$$

Where $\mu_{eff} = \mu + \mu_t$ $\qquad(10)$

$$S = \sqrt{2S_{ij}S_{ij}} \qquad (11)$$

$$S_{ij} = \frac{\partial u_j}{\partial x_i} + \frac{\partial u_i}{\partial x_j} \qquad (12)$$

$$C_{2\varepsilon}^* = C_{2\varepsilon} + \frac{C_\mu\rho\eta^3\left(1-\frac{\eta}{\eta_0}\right)}{1+\beta\eta^3} \qquad (13)$$

$$\eta = S\frac{k}{\varepsilon} \qquad (14)$$

The second order upwind difference scheme was chosen to predict momentum, turbulent kinetic energy and turbulent dissipation rate in each control volume. The SIMPLE algorithm was applied for the iteration procedure.

3. Results and Discussion

3.1 Mean Wall Shear Stress Predictions

Fig. 3 shows the comparison of mean wall shear stress between the numerical data and the experimental data. Both of the numerical data and the experimental data show that mean wall shear stress increases with mean velocity of flow. However, there are some differences between the numerical data and the experimental data.
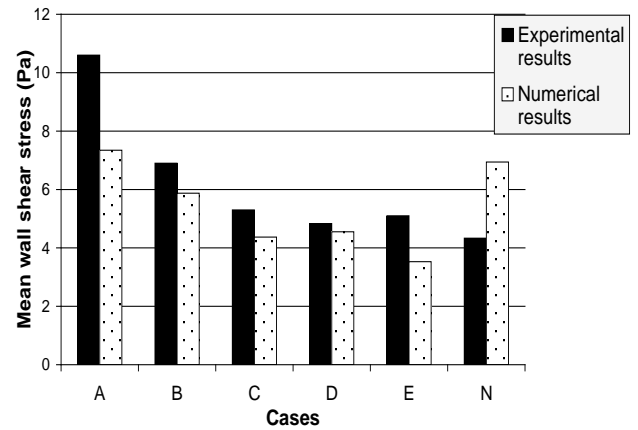

Fig.3 The comparison of mean wall shear stress between the numerical data and the experimental data.

The comparison of mean wall shear stress between pulsed flow (case A) and steady flow (case N) is seen that there is no difference between them when they are analyzed by numerical simulation [12]. Whereas, mean wall shear stress of pulsed flow is higher than mean wall shear stress of steady flow in the experiment. Additionally, for the experimental results, the frequency of pulsations is more effective on mean wall shear stress than the amplitude when the mean velocity is the same (Case C and D). On the other hand, for the

same mean velocity of flow, the amplitude of pulsations is more effective on mean wall shear stress than the frequency when analyzed by numerical simulation as in Fig. 4-5.
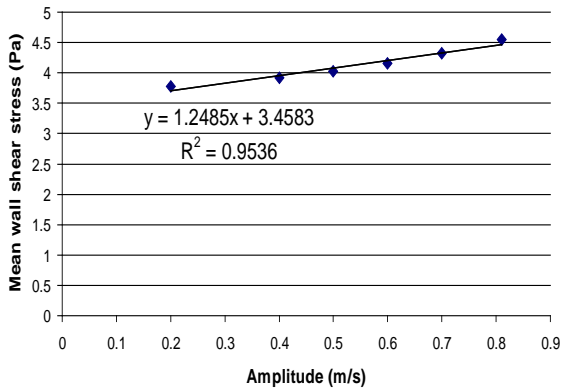

Fig.4 The effect of amplitude of pulsations on mean wall shear stress by numerical simulation.
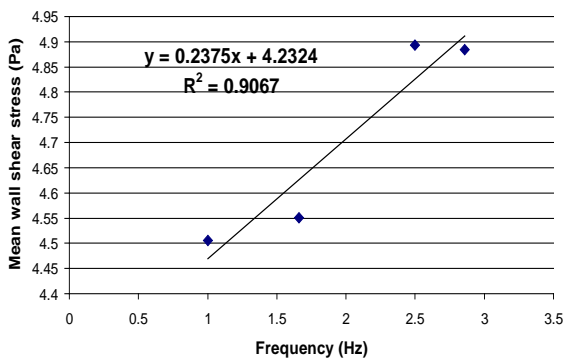

Fig.5 The effect of frequency of pulsations on mean wall shear stress by numerical simulation.

These differences are caused by the difference of the methodology of wall shear stress measurement between the experiment and the simulation. Electrochemical technique [1], which considers mass transfer of the chemical in the flow in form of Sherwood number and transform it into wall shear stress, were used to measure wall shear stress in the experiment. Meanwhile, for the numerical simulation, wall shear stress was obtained by solving the Reynolds-averaged Navier-Stokes equations which does not consider mass transfer of the chemical in the flow.

3.2 Wall Shear Stress Distribution of pulsed flow

Because of the entrance effect, wall shear stress is highest at the inlet of pipe. Then wall shear stress is decreased to the finite value when flow is fully developed as show in Fig. 6. This phenomenon can be seen in every kind of flows, including pulsed flows, except the flow whose velocity is changed immediately such as pulsed flow with square function of velocity inlet. When velocity inlet is change suddenly, there is reverse flow near the wall of pipe. This flow causes the increasing of wall shear stress as in Fig. 7.
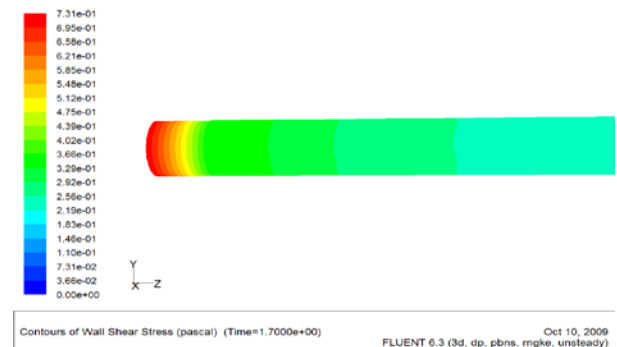

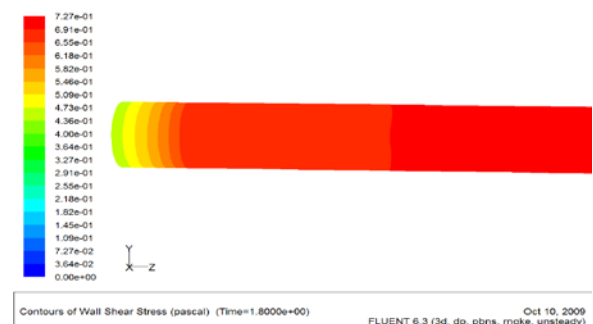Fig.6 Wall shear stress distribution of general pulsed flow in pipe.

Fig.7 Wall shear stress distribution of pulsed flow with square function of velocity inlet at the time that velocity inlet changes suddenly.

3.3 The Effect of Type of Pulsed Flow on Wall Shear Stress by Numerical Simulation

Wall shear stress corresponds to the velocity inlet function as shown in Fig. 8. When the velocity inlet is sine or square function, the variation of wall shear stress with time is sine or square function as well.
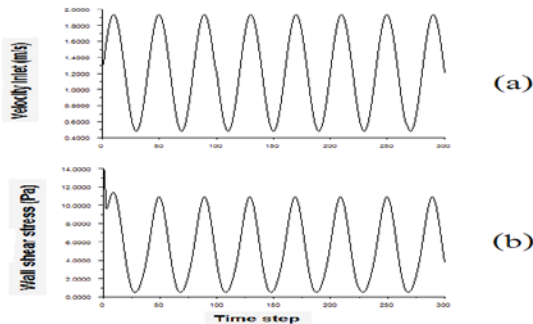

Fig.8 The variation of velocity inlet (a) and wall shear stress (b) with time for sine wave.

There was no effect of type of pulsed flow on mean wall shear stress as shown in Fig. 10. Meanwhile, mean wall shear stress increases with mean velocity inlet, amplitude and frequency of pulsation. Mean velocity inlet is the most effective on the mean wall shear stress as in Fig. 4, 5 and 9. Maximum wall shear stress and frequency of wall shear stress are also proportional to mean velocity inlet, amplitude and frequency of velocity inlet, respectively. Therefore, only wall shear stress analysis is not enough to indicate the cleaning efficiency of different type of pulsed flow. Consequently, the force accumulation on the surface deposit, which is generated by different type of pulsed flow, should be investigated for future work.
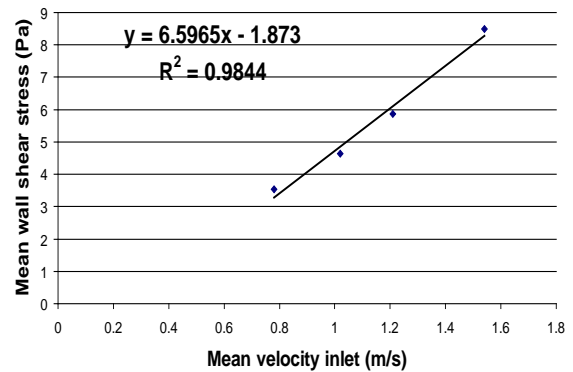

Fig.9 The effect of mean velocity of pulsations on mean wall shear stress by numerical simulation.
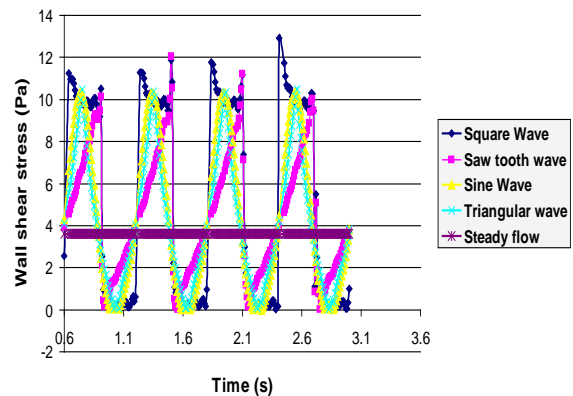

Fig.10 The variation of wall shear stress with time for various type of flow.

4. Conclusion

Wall shear stress of turbulent flow can be calculated by using numerical simulation. But the numerical results are still different from the experimental data because of the difference of the methodology of wall shear stress measurement between the experiment and the simulation. Meanwhile, the numerical simulations of various types of pulsed flow showed that wall shear stress corresponds to the velocity inlet function. Mean wall shear stress is proportional to mean velocity inlet, amplitude and frequency of pulsation. Maximum wall shear stress and frequency of wall shear stress are also

proportional to amplitude and frequency of velocity inlet, respectively.

5. References

[1] Blel, W., Le Gentil-Lelievre, C., Benezech, T., Legrand, J. and Legentilhomme, P. (2009). Application of turbulent pulsating flows to the bacterial removal during a cleaning in place procedure. Part 1: Experimental analysis of wall shear stress in a cylindrical pipe, *Journal of Food Engineering*, vol.90, pp.422-432.

[2] Blel, W., Le Gentil-Lelievre, C., Benezech, T., Legrand, J. and Legentilhomme, P. (2009). Application of turbulent pulsating flows to the bacterial removal during a cleaning in place procedure. Part 2: Effects on cleaning efficiency, *Journal of Food Engineering*, vol.90, pp.433-440.

[3] Changani, S.D., Belmar-Beiny, M.T. and Fryer, P.J. (1997). Engineering and chemical factors associated with fouling and cleaning in milk processing, *Experimental Thermal and Fluid Science*, vol.14, pp.392-406.

[4] Fryer, P.J., Christian, G.K. and Liu, W. (2006). How hygiene happens: physics and chemistry of cleaning, *International Journal of Dairy Technology*, vol.59 (2), May 2006, pp.76-84.

[5] Gillham, C.R., Fryer, P.J., Hasting, A.P.M. and Wilson, D.I. (2000). Enhanced cleaning of whey protein soils using pulsed flows, *Journal of Food Engineering*, vol.46, pp.199-209.

[6] Graßhoff, A. (1983). Die örtliche Flüssigkeitsbewegung und deren Einfluss auf den Renigungsprozess in zylindrischen Toträumen. *Kiel Milchwirtsch. Forxchungsber*, vol. 35,pp.471.

[7] Hinton, A.R., Trinh, K.T., Brooks, J.D. and Manderson, G.J. (2002). Thermophile survival in milk fouling and on stainless steel during cleaning, *Trans IChemE*, vol.80, December 2002, pp.299-304.

[8] Hoffmann, W. and Reuter, H. (1984). Zirkulationsreinigen (CIP) von geraden Rohren in Abhängigkeit on physikalischen Einflußfaktoren. Milchwissenschaft, vol.39,pp.594.

[9] Jackson, A.T. and Low, M.W. (1982). Circulation cleaning of the plate heat exchanger fouled by tomato juice. III. The effect of fluid flow rate on cleaning efficiency, *Journal of Food Technology*, vol. 17,pp.745.

[10] Jun, S. and Puri, V.M. (2005). 3D milk-fouling model of plate heat exchangers using computational fluid dynamics, *International Journal of Dairy Technology*, vol.58(4), November 2005, pp.214-224.

[11] Kakac, S. and Liu, H. (2002). Heat exchangers selection, rating and thermal design, CRc Press, Florida.

[12] Mao, Z. and Hanratty, T. (1986). Studies of the wall shear stress in a turbulent pulsating pipe flow, *Journal of Fluid Mechanic*, vol.170, pp.545-564.

[13] Rosmaninho, R., Rizzo, G., Muller-Steinhagen, H. and Melo, L.F. (2008). Deposition from a milk mineral solution on novel heat transfer surfaces under turbulent flow conditions, *Journal of Food Engineering*, vol.85, pp.29-41.

[14] Timperley, D. (1981). The effect of Reynolds-number and mean velocity of flow on the cleaning in place of pipelines. *In Fundamentals and Applications of Surface Phenomena Associated with Fouling and Cleaning in Food Processing*, Lund University, Lund, Sweden, pp.402.